n-type doping of CuInSe$_2$ and CuGaSe$_2$

Clas Persson,* Yu-Jun Zhao, Stephan Lany, and Alex Zunger

National Renewable Energy Laboratory, Golden, Colorado 80401, USA

The efficiency of CuInSe$_2$ based solar cell devices could improve significantly if CuGaSe$_2$, a wider band gap chalcopyrite semiconductor, could be added to the CuInSe$_2$ absorber layer. This is, however, limited by the difficulty of doping *n*-type CuGaSe$_2$ and, hence, in its alloys with CuInSe$_2$. Indeed, wider-gap members of semiconductor series are often more difficult to dope than lower-gap members of the same series. We find that in chalcopyrites, there are three critical values of the Fermi energy E_F that control *n*-type doping: (i) $E_F^{n,\text{pin}}$ is the value of E_F where the energy to form Cu vacancies is zero. At this point, the spontaneously formed vacancies (=acceptors) kill all electrons. (ii) $E_F^{n,\text{comp}}$ is the value of E_F where the energy to form a Cu vacancy equals the energy to form an *n*-type dopant, e.g., Cd$_{\text{Cu}}$. (iii) $E_F^{n,\text{site}}$ is the value of E_F where the formation of Cd-on-In is equal to the formation of Cd-on-Cu. For good *n*-type doping, $E_F^{n,\text{pin}}$, $E_F^{n,\text{comp}}$, and $E_F^{n,\text{site}}$ need to be as high as possible in the gap. We find that these quantities are higher in the gap in CuInSe$_2$ than in CuGaSe$_2$, so the latter is difficult to dope *n*-type. In this work, we calculate all three critical Fermi energies and study theoretically the best growth condition for *n*-type CuInSe$_2$ and CuGaSe$_2$ with possible cation and anion doping. We find that the intrinsic defects such as V$_{\text{Cu}}$ and In$_{\text{Cu}}$ or Ga$_{\text{Cu}}$ play significant roles in doping in both chalcopyrites. For group-II cation (Cd, Zn, or Mg) doping, the best *n*-type growth condition is In/Ga-rich, and maximal Se-poor, which is also the optimal condition for stabilizing the intrinsic In$_{\text{Cu}}$/Ga$_{\text{Cu}}$ donors. Bulk CuInSe$_2$ can be doped at equilibrium *n*-type, but bulk CuGaSe$_2$ cannot be due to the low formation energy of intrinsic Cu-vacancy. For halogen anion doping, the best *n*-type materials growth is still under In/Ga-rich, and maximal Se-poor conditions. These conditions are not best for halogen substitutional defects, but are optimal for intrinsic In$_{\text{Cu}}$/Ga$_{\text{Cu}}$ donors. Again, CuGaSe$_2$ cannot be doped *n*-type by halogen doping, while CuInSe$_2$ can.

I. INTRODUCTION: THE NEED FOR *n*-TYPE DOPING IN CHALCOPYRITES

Whereas solar cells based on high-cost, vapor-phase epitaxial growth of *single-crystal* III-V semiconductors such as GaInP$_2$/GaAs have high efficiencies [∼32% (Ref. 1)], far less costly solar cells can also be made from simpler growth techniques of CuInSe$_2$ semiconductors, reaching nevertheless efficiencies approaching 20%.[2] An important factor that makes such thin-film CuInSe$_2$ solar cell efficient is that its surface can be type-inverted to become *n*-type even though the bulk of the sample is *p*-type. This is done via deposition of CdS (Refs. 3,4) or ZnS (Ref. 5) or doping in Cd^{2+} electrolyte solution.[6] This leads to band bending. The amount of band bending equals the shift in the Fermi level with respect to the valence band maximum (VBM) from the *p*-type to the *n*-type region. A Fermi level close to the conduction band minimum (CBM), which is needed get the larger band bending, implies, *n*-type conditions at the same time. Thus, both band bending and type inversion are consequences of a common cause, i.e., the increase in E_F at the junction, and are intrinsically tied to each other. To further increase the efficiency, wider band gap materials must be added to the absorber layer. The primary candidate is to add CuGaSe$_2$ ("CGS," band gap $E_g = 1.68$ eV) to CuInSe$_2$ ("CIS," $E_g = 1.04$ eV at room temperature). Unfortunately, as one applies to CuGaSe$_2$ the same process that would convert CuInSe$_2$ to *n*-type (deposition of CdS or ZnS), the Fermi level does not rise towards the CBM. As we will show here, in both CIS and CGS, the formation energy $\Delta H(V_{\text{Cu}}^-)$ of the Cu vacancy is lowered as E_F moves towards the CBM. Once E_F crosses a point $E_F^{n,\text{pin}}$ where $\Delta H(V_{\text{Cu}}^-) \approx 0$, Cu atoms leave the lattice spontaneously. Since such Cu vacancies are acceptors which capture free electrons, once $E_F = E_F^{n,\text{pin}}$ the Fermi level can no longer rise towards the CBM. The question is then why in CIS, treatment by *n*-type dopants does move the E_F towards the CBM, but similar treatment does not have this effect in CGS. In other words, how different is $E_F^{n,\text{pin}}$ in CIS vs CGS. The inability to shift E_F upwards in CGS poses a severe limitation on making solar cells that contain a wide-gap CGS layer, or a Ga-rich CuIn$_{1-x}$Ga$_x$Se$_2$ alloy layer. Indeed, considering a series of compounds with decreasing band gaps such as AlN→GaN→InN or C→Si→Ge, it is often difficult to *n*-type dope the member with the wider gap. In this paper we enquire theoretically, using first-principles methods, what are the reasons that divalent cation dopants such as Mg, Zn, and Cd or anion-site dopants such as Cl, Br, I, do not type-convert CGS, while they do type-convert CIS. We also provide an Appendix describing a practical scheme on how state-of-the-art defect calculations can be done. We conclude that *n*-type doping of CuGaSe$_2$ is impossible under equilibrium conditions, but could be possible if one could prevent Cu outdiffusion at high E_F via nonequilibrium effects.

II. GENERAL PHYSICS OF DEFECTS FORMATION ENERGIES

A. Dependence on E_F and μ, and the "Doping Rules"

Formation of defects can be viewed as a process in which a certain number of atoms and electrons are exchanged be-

tween the host material and some atomic and electronic reservoirs.[7] Thus, the formation energy for a defect comprising of atoms α in the charge state q can be computed using the expression[8,9]

$$\Delta H_{D,q}(E_F,\mu) = (E_{D,q} - E_H) + \sum_\alpha n_\alpha \mu_\alpha + q(E_v + E_F). \quad (1)$$

In the first term, $E_{D,q}$ and E_H are the total energies of a solid with and without defect D, respectively. The second term of Eq. (1) represents the energy change due to exchange of atoms with the chemical reservoirs. μ_α is the absolute value of the chemical potential of atom α, and n_α is the number of such defect atoms; $n_\alpha = -1$ if an atom is added, while $n_\alpha = 1$ if an atom is removed. For example, the energy $\Delta H_{D,q}(E_F,\mu)$ to introduce a $D = V_{Cu}$ (Cu vacancy) is higher the greater is the Cu chemical potential μ_{Cu}, since the Cu atom ejected from the solid upon forming V_{Cu} must join the Cu reservoir whose energy is μ_{Cu}. The third term in Eq. (1) represents the energy change due to exchange of electrons and holes with the carrier reservoirs. E_v represents the energy at the VBM of the defect free system, i.e., the energy to remove an electron from the VBM to Fermi reservoir, or to insert an electron from the Fermi reservoir. E_F is the Fermi energy relative to the E_v. In a non-degenerate semiconductor, E_F is bound between E_v and the CBM, E_c. One can qualitatively understand the $(E_v + E_F)$ dependence of $\Delta H_{D,q}(E_F,\mu)$ in Eq. (1) as follows: The energy needed to form a positively-charged defect (donors) increase the higher is E_F in the gap, because the electron ejected upon forming the positive defect must join the electron reservoir whose energy is E_F. Conversely, the energy needed to form negatively-charged defects (acceptors) is smaller the higher is E_F in the band gap.

Since the defect formation energies are conventionally defined with respect to the chemical potential of the elemental solid(s), we express μ_α as $\mu_\alpha = \mu_\alpha^{solid} + \Delta\mu_\alpha$. Equation (1) can thus be rewritten as

$$\Delta H_{D,q}(E_F,\mu) = (E_{D,q} - E_H) + \sum_\alpha n_\alpha(\Delta\mu_\alpha + \mu_\alpha^{solid})$$

$$+ q(E_v + E_F). \quad (2)$$

The relevance of Eq. (2) to doping is that the equilibrium concentration of defect D in charge state q depends on the Boltzmann factor $\exp[-\Delta H_{D,q}(E_F,\mu)/kT]$. Thus, all other things being equal, positively charged defects (electron-producing donors) have higher concentration in p-type environment (E_F near E_v), whereas negatively charged defects (hole-producing acceptors) have higher concentration in n-type environment (E_F near E_c). Furthermore, cation-substituting impurities have higher concentrations under cation-poor growth condition ($\Delta\mu_{cation}$ most negative), whereas anion-substituting impurities have higher concentrations under anion-poor growth conditions ($\Delta\mu_{anion}$ most negative).

These considerations can be summarized in the form of "doping rules"[10] for n-type chalcopyrite shown in Fig. 1. These rules determine which growth conditions, according to Eq. (2) minimize the formation energies ΔH of wanted de-

	Anion-site doping (e.g. CIS : Cl)	Cation-site doping (e.g. CIS : Cd)
(1) To maximize dopant solubility use:	• Dopant-rich • Anion-poor	• Dopant-rich • Cu-poor
(2) Competing phases are: To reduce effect use:	Dopant + host-*cation* (e.g. CuCl, InCl) • Cation-poor (=Anion-rich)	Dopant + host-*anion* (e.g. CdSe) • Anion-poor (=Cation-rich)
(3) Electron-killer is: To minimize electron killers V_{Cu} use:	V_{Cu}^- • Cu-rich	V_{Cu}^- • Cu-rich
(4) Assisting intrinsic defect is: To maximize assisting In_{Cu} use:	In_{Cu}^{2+} • In-rich • Cu-poor	In_{Cu}^{2+} • In-rich • Cu-poor
(5) "wrong site" defects are: To minimize "wrong site" defects use:	—	Cd_{Cu}^+ vs. Cd_{In}^- • Cu-poor • In-rich

FIG. 1. n-type doping rules for CIS and CGS. The terms "anion" and "cation" refer to the *host* atoms, i.e., Cu, In, Ga, and Se.

fects, and maximize ΔH of unwanted defects. We illustrate in the following these rules (Fig. 1 exemplified for Cd doping in CIS):

(1) *Solubility*: Maximal incorporation of Cd into the CIS lattice requires lowering $\Delta H(Cd_{Cu})$. This means, according to Eq. (2), Cu-poor (i.e., low $\Delta\mu_{Cu}$) and dopant-rich (i.e., maximal $\Delta\mu_{Cd}$) growth conditions.

(2) *Competing phases:* The formation of unwanted dopant-host compounds, such as CdSe, lowers $\Delta\mu_{dopant}$ by consuming Cd. To maintain maximal $\Delta\mu_{dopant}$ needed in Rule (1), one needs to maintain host-anion poor (i.e., low $\Delta\mu_{Se}$, i.e., host-cation rich) growth conditions.

(3) *Killer defects:* The Cu vacancy V_{Cu}^- is an acceptor, which compensates the intended donor doping. By Eq. (2), its formation energy $\Delta H(V_{Cu})$ is lowered as the Fermi energy rises in the band gap toward E_c. We define a special Fermi energy $E_F^{n,pin}$, as the value where $\Delta H(V_{Cu}^-; E_F) = 0$. At this point any further donor doping is compensated by the spontaneous formation of V_{Cu}^-. For successful doping, $E_F^{n,pin}$ needs to be as high as possible in the gap. This requirement of minimizing the concentration of V_{Cu} requires Cu-rich growth conditions ($\Delta\mu_{Cu} = 0$).

(4) *Assisting defects:* The antisite In_{Cu}^{++} or Ga_{Cu}^{++} is a (double) donor which, when formed, ejects electrons, thus assists the intended n-type doping. By Eq. (2), its formation energy $\Delta H(In_{Cu}^{++})$ is lowered as the Fermi energy moves down in the gap towards E_v. At the Fermi energy $E_F^{n,comp}$ we have $\Delta H(V_{Cu}^-; E_F) = \Delta H(In_{Cu}^{++}; E_F)$ at which point the intrinsic donors compensate the intrinsic acceptors. For successful n-type doping, $E_F^{n,comp}$ needs to be as high as possible in the gap. This requires In-rich conditions, i.e., high $\Delta\mu_{In}$.

(5) *Wrong-site substitution: n*-type doping by divalent cation requires Cd-on-Cu substitution (a donor), i.e., low $\Delta H(Cd_{Cu}^+; E_F)$, but is hampered by Cd-on-In substitution (an acceptor), i.e., by low $\Delta H(Cd_{In}^-; E_F)$. The Fermi level denoted by $E_F^{n,site}$ is the point where $\Delta H(Cd_{Cu}^+) = \Delta H(Cd_{In}^-)$. For successful n-type doping, $E_F^{n,site}$ needs to be as high as pos-

sible in the gap. This requires Cu-poor and In-rich (Se-poor) conditions.

In order to study the limitations of *n*-type doping, we first determine the optimum growth conditions for *n*-type doping in CIS and CGS. We note that, considering an extended range of chemical potentials, Rules (1)–(5) impose intrinsically conflicting requirements, e.g., the Cu-rich conditions required by Rule (3) conflict with Rules (1), (4), and (5) in case of Cd doping. However, only a limited range of chemical potentials of the host atoms is allowed thermodynamically. We therefore must establish next the thermodynamic limit on $\Delta\mu_{Cu}$, $\Delta\mu_{In/Ga}$, and $\Delta\mu_{Se}$, and examine then if Rules (1)–(5) of Fig. 1 can be accommodated with no conflicts within the limited, *allowed* range of $\{\Delta\mu\}$.

B. Restrictions posed by equilibrium chemical potentials

The chemical potentials μ_α are bound by the values that maintain a stable host compound, and avoid formation of all other competing phase (including their elemental solids). We will formulate these conditions in four steps. The procedure is based on equilibrium conditions for the crystal growth. When a nonequilibrium process is proposed, some constrains should be re-evaluated.

(i) The atomic chemical potential should be smaller than that of the corresponding elemental solid to avoid precipitation of the latter. That is:

$$\Delta\mu_{Cu} \leq 0; \quad \Delta\mu_{In,Ga} \leq 0; \quad \Delta\mu_{Se} \leq 0; \quad (3)$$

or

$$\mu_{Cu} \leq \mu_{Cu}^{solid}; \quad \mu_{In,Ga} \leq \mu_{In,Ga}^{solid}; \quad \mu_{Se} \leq \mu_{Se}^{solid}. \quad (4)$$

The point $\mu_\alpha = \mu_\alpha^{solid}$, corresponds to a "maximum α-rich condition," i.e., the chemical potential of α is equilibrium with elemental α solids.

(ii) To maintain a stable compound the sum of chemical potentials of its constituent atoms must equal the heat of formation of the compound. That is

$$\Delta\mu_{Cu} + \Delta\mu_{In,Ga} + 2\Delta\mu_{Se} = \Delta H(\text{Cu(In,Ga)Se}_2); \quad (5)$$

or

$$\mu_{Cu} + \mu_{In,Ga} + 2\mu_{Se} = \Delta H(\text{Cu(In,Ga)Se}_2) + \mu_{Cu}^{solid} + \mu_{In,Ga}^{solid} + 2\mu_{Se}^{solid}. \quad (6)$$

(iii) The chemical potentials are further restricted by requiring that, other possible competing phases with Cu, (In,Ga), and Se do not form. For example, if Cu and Se forms Cu$_m$Se$_n$ naturally, the following condition is applied:

$$m\Delta\mu_{Cu} + n\Delta\mu_{Se} \leq \Delta H(\text{Cu}_m\text{Se}_n). \quad (7)$$

The higher the number of conditions one adds to avoid competing phases, the more realistic is the region of the atomic potentials. For CIS we consider as competing phases InSe (having mP8 structure in Pearson's symbol), Cu$_3$Se$_2$ (the tP10 structure), and CuIn$_5$Se$_8$ (type D in Ref. 10), while for CGS we consider GaSe (the hP8 structure), Cu$_3$Se$_2$, and CuGa$_5$Se$_8$ (same structure as CuIn$_5$Se$_8$). All of these formation enthalpies are calculated theoretically using LDA, as described in Sec. III.

(iv) Additional constrains are posed by the possibility of forming compounds between the dopant atoms and the host atoms. We thus require for halogen doping (exemplified by Cl) in CIS

$$\Delta\mu_{In} + \Delta\mu_{Cl} \leq \Delta H(\text{InCl}), \quad (8)$$

$$\Delta\mu_{Cu} + \Delta\mu_{Cl} \leq \Delta H(\text{CuCl}), \quad (9)$$

whereas for divalent doping (exemplified by Cd) in CIS we require:

$$\Delta\mu_{Cd} + \Delta\mu_{Se} \leq \Delta H(\text{CdSe}). \quad (10)$$

$$\Delta\mu_{Cd} + 2\Delta\mu_{In} + 4\Delta\mu_{Se} \leq \Delta H(\text{CdIn}_2\text{Se}_4)$$

For CGS we have analogous conditions for Ga$_2$Cl$_6$, CuCl, CdSe, and CdGa$_2$Se$_4$. The structure assumed in calculating their ΔH values are InCl (red crystal phase, see Ref. 11); CuCl (zinc-blende); CdSe (zinc-blende); CdIn$_2$Se$_4$ (pseudocubic); CdGa$_4$Se$_4$ (tetragonal); Ga$_2$Cl$_6$ (gas phase[12]).

Figures 2(a) and 2(b) show the computed chemical potential domains for CIS and CGS resulting from conditions (i)–(iii). The shaded areas are the allowed chemical potential ranges for the chalcopyrites. In the white regions, the chalcopyrites are unstable with respect to the competing phases shown in the figures. For example, the white area at the bottom right corner of Fig. 2(a) are excluded due to the precipitation of Cu$_2$Se$_3$, CuSe, and Cu$_2$Se. The white areas on the left are excluded due to the formation of III-Se compounds[13] and the ordered defect structures.

C. Selecting optimal growth conditions: Cd, Zn, Mg, in CIS and CGS

Having calculated the allowed regions of $\{\mu_{Cu}; \mu_{In/Ga}; \mu_{Se}\}$, we are now in a position to select points in this plane of Fig. 2 that represent the best compromise with the "doping rules" of Fig. 1. Taking into account these restrictions, Fig. 3 shows for CIS the dependence of the defect formation energies on the growth conditions described by $\Delta\mu_{Cu}$ and $\Delta\mu_{In}$ [the dependence on $\Delta\mu_{Se}$ is implicitly contained via Eq. (5)]. We see that maximally Se-poor conditions (denoted "point N" in Fig. 3), fulfill the following requirements in case of Cd-doping: (1) Fig. 3(a) shows that $\Delta H(\text{Cd}_{Cu})$ is minimal at "point N" [as required by Rule (1) of maximal solubility of Cd$_{Cu}$]; (2) Fig. 3(c) shows that $\Delta H(V_{Cu})$ is maximal at "point N" [as required by Rule (3)]; (3) Fig. 3(d) shows that $\Delta H(\text{In}_{Cu})$ is minimal at "point N" [as required by Rule (4)]; An analogous argument can be made for CGS. Thus, these Se-poor conditions satisfy the doping Rules (1)–(4), and resolve most of the conflicts indicated by Fig. 1. The "point N" conditions are defined by the chemical potentials listed in Table I. The corresponding maximal chemical potentials of Mg and Zn at "point N" are -1.40 eV, -0.45 eV for CIS, and -1.37 eV, -0.42 eV for CGS, as collected in Table I. According to Rule (1), we used Fig. 3 the maximal Cd chemical potential allowed by Eqs.
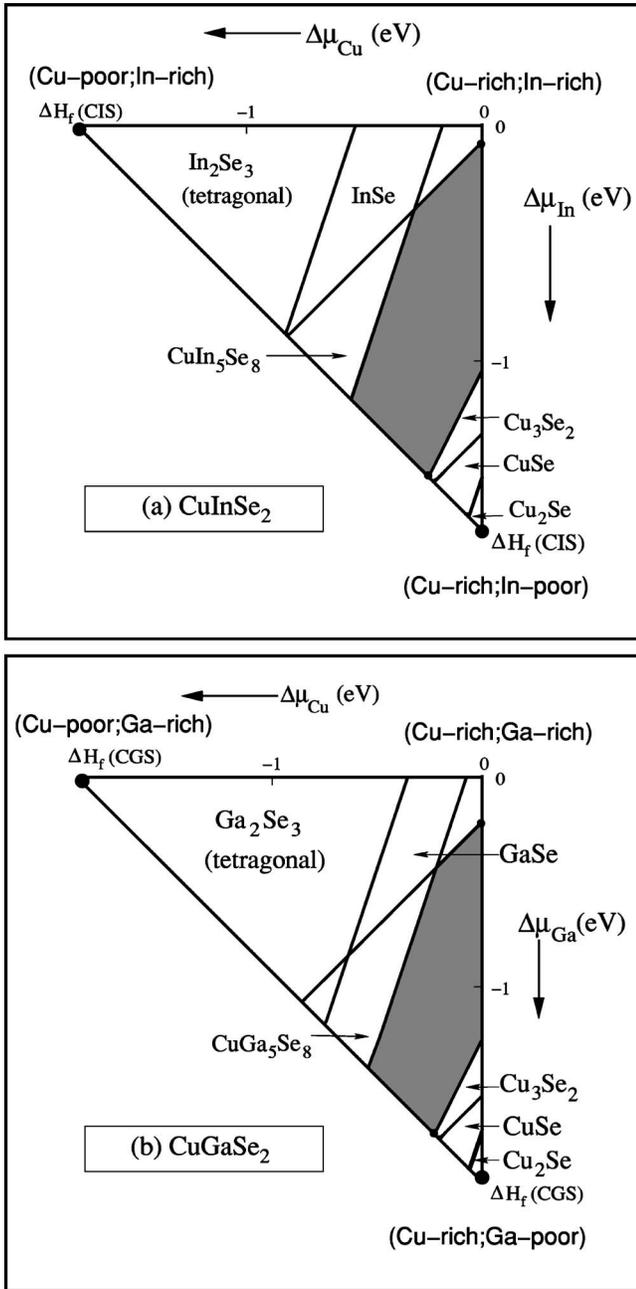
FIG. 2. The allowed chemical potential domains (shaded area) for (a) CIS and (b) CGS, shown in the $(\Delta\mu_{Cu}, \Delta\mu_{III})$ plane. The white regions are areas which are excluded due to the formation of competing phases specified in the figures.

FIG. 3. (Color online) Contour plot of the defect formation energies ΔH in CIS, illustrating the dependence on chemical potentials $\Delta\mu_{Cu}$ and $\Delta\mu_{In}$ (dependence on $\Delta\mu_{Se}$ is implicit). Dark shading corresponds to low ΔH (high concentration), light shading to high ΔH (low concentration). The contour spacing corresponds to 0.1 eV. the ideal choices, according to the rules of Fig. 1 are: (a) Minimize $\Delta H(Cd_{Cu})$ for Cd-doping [Rule (1)]. (b) Minimize $\Delta H(Cl_{Se})$ for Cl-doping [Rule (1)]. (c) Maximize $\Delta H(V_{Cu})$ [Rule (3)]. (d) Minimize $\Delta H(In_{Cu})$ [Rule (4)]. (e) Maximize $\Delta H(Cd_{In})$ [Rule (5)].

(10). Thus $\Delta\mu_{Cd}$ is limited by formation of CdSe for Cu-rich conditions (right part of the allowed range, e.g., $\Delta\mu_{Cu}=0$), and by formation of $CdIn_2Se_4$ for more Cu-poor conditions (left part of the allowed range). This leads to the "kinks" in the contour plots of Figs. 3(a) and 3(e). We see in 3(e) that the maximal $\Delta H(Cd_{In})$ required by Rule (5) is obtained at "point Q", which conflicts with Rules (1), (3), and (4) requiring "point N" growth conditions. However, using the maximal Cd chemical potential leads to undesirably high Cd incorporation (cp. Sec. IV) in either case, e.g., the formation of CdSe-CuInSe$_2$ solid solutions, at point N. Thus, we use be-

low a reduced value for $\Delta\mu_{Cd}$, which yields defect concentrations more suitable for the purpose of doping. Experimentally, such a reduction of $\Delta\mu_{Cd}$ may be obtained by supplying only a limited amount of Cd. Due to the choice of a reduced $\Delta\mu_{Cd}$ for the extrinsic dopand Cd, the optimal growth conditions are now governed by the Rules (3) and (4), which concern the intrinsic defects. According to these rules, we find that "point N" growth conditions, i.e, Cu-rich, In-rich, and Se-poor, constitute the optimal choice for n-type doping with divalent atoms. Thus we regard only these growth conditions for Cd-doping in the following.

TABLE I. Chemical potentials ($\Delta\mu$ in eV) for the host atoms and the group II atoms in CIS and CGS at "point N" (cf. Fig. 3): Cu-rich, In/Ga-rich, maximally Se-poor, and group-II dopants rich.

	$\Delta\mu_{Cu}$	$\Delta\mu_{In}/\Delta\mu_{Ga}$	$\Delta\mu_{Se}$	$\Delta\mu_{Mg}$	$\Delta\mu_{Zn}$	$\Delta\mu_{Cd}$
CIS	0	−0.07	−0.83	−1.40	−0.45	−0.21
CGS	0	−0.21	−0.86	−1.37	−0.42	−0.18

D. Selecting optimal growth conditions for Cl, Br, I in CIS and CGS

In the case of anion-site doping, some of the conflicting requirements noted in Fig. 1 do remain, even if we consider the restricted chemical potential range. Figure 3(b) shows the contour plot for $\Delta H(Cl_{Se})$, where $\Delta\mu_{Se}$ is maximized as far as allowed by Eqs. (8) and (9). Comparing Figs. 3(b)–3(d), we see that minimal $\Delta H(Cl_{Se})$ required by Rule (1) is obtained at "point P," but maximal $\Delta H(V_{Cu})$ and minimal $\Delta H(In_{Cu})$, as required by Rules (3) and (4), are both fulfilled only at point N. We thus decided to use two different growth conditions. Under the first strategy ("point P") we will maximize the concentration of halogen, thus following Rule (1). This is consistent with Rules (2) and (3), but conflicts with Rule (4). We will refer to this as "*halogen favored conditions*," and "Cl$_{Se}$ favored conditions" when the halogen dopant is Cl. This gives values collected in Table I. "Point P" corresponds to "Se, In intermediate, Cu-rich."

Under the second strategy ("point N") we minimize $\Delta H(In_{Cu})$ according to Rule (4), which is referred as "In$_{Cu}$ *favored conditions*." Under these conditions, the Cl chemical potentials are limited by InCl and Ga₂Cl₆ formation ($\Delta\mu_{Cl}$ =−1.74 eV in CIS, and $\Delta\mu_{Cl}$=−1.47 eV in CGS, given with respect to the diatomic Cl molecule, i.e., $\mu_{Cl}^{solid}=\frac{1}{2}\mu_{Cl_2}$). Analogously, the maximal chemical potentials of Br and I at "point N" are −1.53 eV, −1.27 eV in CIS, as listed in Table II. "Point N" growth conditions corresponds to Cu-rich (equilibrium with metallic Cu), In- or Ga-rich (equilibrium with InSe or GaSe), and Se-poor.

III. METHOD OF CALCULATING $\Delta H_{D,q}(E_F;\mu)$

A. Formation energies

The present computational method for determining the formation energies and the transition energies of neutral and charged divalent donors and acceptors in Cu(In,Ga)Se₂ are based on the projector augmented wave (PAW) potentials within the local density approximation (LDA),[14] using the relaxed LDA crystal lattice parameters a=5.789 Å and c/a =1.980 for CIS, and a=5.537 Å and c/a=1.970 for CGS. The total energies of neutral and charged doped Cu(In,Ga)Se₂ systems are calculated using 64 atoms simple-cubic supercells and a Γ centered **k**-mesh containing six special **k**-points. The charge density is obtained from the corrected tetrahedron **k**-space integration method[14] with an energy cutoff of 400 eV. The atom positions are fully relaxed for both the neutral and the charged dopants. The chemical potentials of the elemental solids are obtained from fully converged LDA/PAW total energy calculations.

The procedure for calculating defect formation energy from Eqs. (1) and (2) involves a number of crucial technical issues that are often overlooked. These can cause significant differences in the results, even if the cell size, LDA approximation, and convergence parameters are the same. We present in the Appendix a detailed technical description of the main issues to be dealt with in LDA supercell calculations of defects energies. Here, we briefly describe the physics behind these five corrections.

(i) *Determining the valence-band maximum*: In principle, the E_v in Eqs. (1) and (2), should be determined from total

TABLE II. Chemical potentials ($\Delta\mu$ in eV) for the CIS and CGS host atoms and the halogen atoms for "halogen favored" conditions [point P in Fig. 3(b)] and for "In$_{Cu}$ favored" conditions (point N). Point P is Cu-rich, In- and Se-intermediate, and halogen rich. Point N is Cu-rich, In-rich, maximally Se-poor, and halogen rich.

CIS	$\Delta\mu_{Cu}$	$\Delta\mu_{In}$	$\Delta\mu_{Se}$	$\Delta\mu_{Cl}$	$\Delta\mu_{Br}$	$\Delta\mu_{I}$
Cl$_{Se}$ favored (P)	0	−0.70	−0.51	−1.11		
Br$_{Se}$ favored (P)	0	−0.70	−0.51		−0.90	
I$_{Se}$ favored (P)	0	−0.63	−0.55			−0.77
In$_{Cu}$ favored (N)	0	−0.07	−0.83	−1.74	−1.53	−1.27
CGS	$\Delta\mu_{Cu}$	$\Delta\mu_{Ga}$	$\Delta\mu_{Se}$	$\Delta\mu_{Cl}$	$\Delta\mu_{Br}$	$\Delta\mu_{I}$
Cl$_{Se}$ favored (P)	0	−1.29	−0.32	−1.11		
Br$_{Se}$ favored (P)	0	−0.53	−0.70		−0.90	
I$_{Se}$ favored (P)	0	−0.33	−0.80			−0.77
Ga$_{Cu}$ favored (N)	0	−0.21	−0.86	−1.47	−1.22	−0.89

energy difference between the neutral host and the host with a VBM electron removed. We found that the energy difference converges to the eigenvalue of VBM, $\varepsilon_{\mathrm{VBM}}$, in the limit of dilute hole concentration. Therefore, $\varepsilon_{\mathrm{VBM}}$ could be used as the value of VBM for the diluted defects along with a potential alignment between two supercell calculations. This is described in Sec. 1 in the Appendix.

(ii) *LDA energy gap correction*: The LDA underestimates the fundamental band-gap energies of semiconductors. This LDA error will also be reflected in underestimated donor and acceptor single-particle eigenstates. Traditionally, one corrects the LDA band-gap error by keeping the energy of the VBM fixed, and shifting upwards the conduction bands. This approximation may hold for most common semiconductors. However, Cu-III-VI$_2$ have strong Cu, d character at the VBM, and it is well known that LDA does not describe d-states accurately.[15] For example, the LDA Cu, d resonance inside the valence band has a too low binding energy relative to photoemission.[16] Using the LDA+U method, and applying an on-site Coloumb energy for Cu of $U_d(\mathrm{Cu})=6$ eV on the Cu, d-like states, results in a downward energy shift of 0.37 eV for both CIS and CGS. With this potential correction, the Cu, d-like valence band resonances agrees better with photoemission measurements.[17] We therefore correct the band-gap energy by a shifting the VBM downward by 0.37 eV in both CIS and CGS. To set the experimental gaps of 1.04 and 1.68 eV in CIS and CGS we add an upwards energy shift of the CBM 0.58 eV and 1.03 eV in CIS and CGS, respectively. This is described in Sec. 2 of the Appendix.

(iii) *Band filling correction*: The use of finite supercell entails two types of corrections: the band-filling correction and an image charge correction. In a finite supercell, the impurity-impurity interaction forms an impurity band instead of a single donor (or acceptor) eigenstate. The donor electrons (or acceptor holes) now also populates states with higher energies compared to the single donor (acceptor) state in the dilute limit. Thus, one has to correct the total energy of the finite supercell due to this band dispersion and band-filling effects. The correction is ~0.7–0.9 eV for the present divalent donors in Cu(In,Ga)Se$_2$ and ~0.06–0.13 eV for the acceptors. This is described in Sec. 3 of the Appendix.

(iv) *Potential alignment correction for charged defects (any cell size)*: The calculation of the total energy of a system containing a charged donor (or a charged acceptor) may not necessarily refer to the correct host crystal potential, since ionizing the donor (acceptor) means removal of one electron from (adding one electron to) the system. We determined the potential alignment from the deeply lying III-d state which has a sharp density-of-state peaks at ~15 eV below the VBM. This potential alignment yields a correction to the total energy by ~0.05–0.25 eV in the present calculations. This is described in Sec. 4 in the Appendix.

(v) *Image charge corrections due to finite supercell (charged defects only)*: A finite supercell which contains a charged donor or a charged acceptors, usually implies[18] multipole interaction between the close-lying equivalent supercells. This multipole interaction according to Makov and Payne,[18] could yield a correction in the order of ~0.1 eV for the present divalent dopants. We present the calculated for-

mation energies and corresponding transition energies both with and without the multipole correction. However, the defect levels calculated here are rather shallow, having extended wave functions, we do not use the truncated multipole expansion of Ref. 18 for the image charge correction, i.e., we use the values of defect formation energies without image charge correction for calculating the defect and carrier concentrations. This is described in Sec. 5 of the Appendix.

B. Electronic transition energy

The transition energy $\varepsilon(D, q/q')$ is defined as the Fermi energy at which the charge state of defect D spontaneously transform $q \leftrightarrow q'$. Thus, the transition energy is the Fermi energy for which $\Delta H(D, q) = \Delta H(D, q')$. From Eq. (2) one obtains:

$$\varepsilon(D, q/q') = \frac{E(D, q) - E(D, q')}{q' - q} - E_v. \quad (11)$$

In the Appendix, we described the procedure for calculating the VBM and $E(D, q)$ using the LDA finite supercell approach, which requires certain corrections. No additional corrections are required for the transition energies.

C. Self-consistent determination of concentrations

The equilibrium defect concentration is calculated from the defect formation energies, according to Boltzmann distribution

$$c_{D,q}(E_F, \mu_\alpha, T) = N \exp[-\Delta H_{D,q}(E_F, \mu_\alpha)/kT], \quad (12)$$

where N is the concentration of atomic sites that are substituted by the defect, the chemical potentials μ_α correspond to the growth conditions described above, and T is the temperature used in the growth of solar cell devices. We used here $T=800$ K.[19] Since the defect concentrations depend explicitly on E_F, and, in turn, E_F depends on the concentrations of the charged defects and the free carriers (via the requirement of overall charge neutrality), we determine self-consistently $\{c_{D,q}; E_F;$ carrier concentration$\}$. Here, the electron and hole concentrations are calculated as a function of E_F and T by numerical integration of the Fermi-Dirac distribution function using an effective-mass like approximation for the host bands.[20]

Using the self-consistently calculated defect concentrations, we define the "net doping balance"

$$\Delta c = c_{\mathrm{Cl}_{\mathrm{Se}}} + 2c_{\mathrm{In}_{\mathrm{Cu}}} - c_{\mathrm{V}_{\mathrm{Cu}}}, \quad (13)$$

in the case of Cl doping, and

$$\Delta c = c_{\mathrm{Cd}_{\mathrm{Cu}}} + 2c_{\mathrm{In}_{\mathrm{Cu}}} - c_{\mathrm{Cd}_{\mathrm{In}}} - c_{\mathrm{V}_{\mathrm{Cu}}}, \quad (14)$$

in the case of Cd doping. Here, defect concentrations include all possible charge states as the charge state index q is not shown. The doping balance Δc indicates whether net donor doping ($\Delta c > 0$) or net acceptor doping ($\Delta c < 0$) is obtained
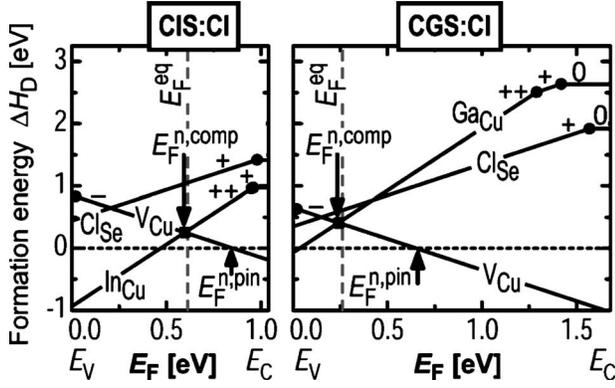
FIG. 4. Cl$_{Se}$ and related defect formation energies under "point N" growth conditions. $E_F^{n,comp}$ indicates the Fermi energy where ΔH of the donor In$_{Cu}^{++}$ (Ga$_{Cu}^{++}$) and the acceptor V$_{Cu}^-$ intersect. The vertical line indicates the self-consistently calculated equilibrium Fermi energy E_F^{eq} at $T=800$ K.

FIG. 5. Cd$_{Cu}$ and related defect formation energies under "point N" growth conditions. $E_F^{n,site}$ indicates the Fermi energy where ΔH of the donor Cd$_{Cu}^+$ and the acceptor Cd$_{In}^-$ (Cd$_{Ga}^-$) intersect. The vertical line indicates the self-consistently calculated equilibrium Fermi energy E_F^{eq} at $T=800$ K.

(In$_{Cu}$ is a double donor and, accordingly contributes $2c_{In_{Cu}}$ to Δc). On account of the charge neutrality condition, the self-consistent equilibrium Fermi energy E_F^{eq} is pinned around $E_F^{n,comp}$ in case of Cl doping [Fig. 4]. For n-type doping, E_F^{eq} generally needs to be high in the gap.

In order to compare our results with measured electron concentrations for Cl and Cd doping in CIS, we perform an additional self-consistent calculation for room temperature ($T=300$ K). It is assumed that due to kinetic barriers, the total defect concentrations at $T=300$ K, including all charge states, is frozen-in at the values calculated for 800 K. For self-consistent solution, however, we use now $T=300$ K to calculate carrier density according to the Fermi-Dirac distribution. Also, the ration between the concentrations of the different charge states of the defects is calculated according to the Boltzmann distribution at 300 K.

IV. DEPENDENCE OF ΔH ON E_F AND CRITICAL VALUES OF THE FERMI ENERGY

As the doping rules of Fig. 1 suggest, the main defect formation events controlling doping are formation of killer defects [Rule (3)], of assisting defects [Rule (4)], and wrong-site defects [Rule (5)]. There are corresponding critical values of the Fermi energy associated with these events. Figure 4 shows ΔH vs E_F for Cl doping, whereas Fig. 5 gives analogous results for Cd doping. Tables III and IV give the calculated formation energies for divalent and halogen dopants, respectively.

A. Spontaneous formation of killer defects

The Fermi energy where $\Delta H(V_{Cu}^-; E_F)=0$ is denoted $E_F^{n,pin}$; ideally, it should be as high in the band gap (or inside the conduction band) as possible for then free electrons can be formed before they are destroyed by the reaction $V_{Cu}^0 + e \rightarrow V_{Cu}^-$. Figure 4 shows that the energy needed to form V_{Cu} when E_F is close to the VBM is rather similar in CIS and CGS. This reflects the fact that in both materials the valence band is constructed mostly from Cu d and Se p orbitals with-

out participation of Ga or In. This is illustrated in the calculated density of states (DOS) in Fig. 6. This is also reflected by the existence of a small[21] valence band offset between CIS and CGS, and a similar Cu-Se bond length in both materials.[16] However, Fig. 4 also shows that $E_F^{n,pin}$ occurs in CIS rather close to the CBM, making this material n-type dopable, whereas in CGS the pinning level is below midgap, suggesting that electron killers form spontaneously before the Fermi level has a chance of approaching the conduction band. The main reason for this difference is the fact that the CBM in CGS is higher in energy (closer to vacuum) than in CIS.[10]
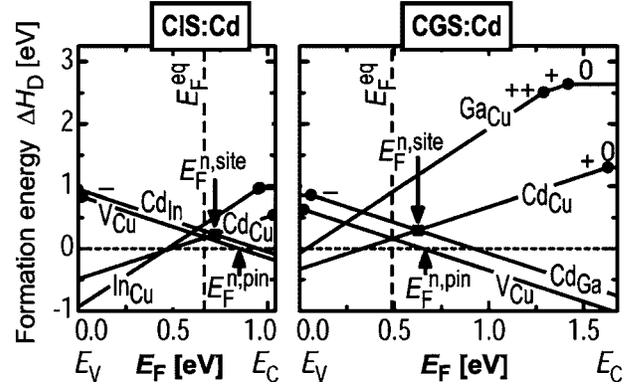
B. Formation of assisting defects

The Fermi energy where the lowest intersection point between donors and acceptors, is denoted $E_F^{n,comp}$; ideally, it

TABLE III. Formation energies ΔH of substantial neutral and charged group-II donors and acceptors in CIS and CGS. The Fermi energy E_F is relative to the VBM E_v. Values within bracket are the formation energies in the absence of the Makov-Payne correction.

	$\Delta H(D,q)$ [eV]		
	$[E(D,q)-E(0)]+\Sigma_\alpha n_\alpha \mu_\alpha^{solid}$		$\Sigma_\alpha n_\alpha \Delta \mu_\alpha + q(E_v+E_F)$
	CuInSe$_2$	CuGaSe$_2$	
Mg$_{Cu}^0$	-1.22	-0.25	$-\Delta\mu_{Mg}+\Delta\mu_{Cu}$
Zn$_{Cu}^0$	-0.11	$+0.71$	$-\Delta\mu_{Zn}+\Delta\mu_{Cu}$
Cd$_{Cu}^0$	$+0.13$	$+1.12$	$-\Delta\mu_{Cd}+\Delta\mu_{Cu}$
Mg$_{III}^0$	-0.65	-0.49	$-\Delta\mu_{Mg}+\Delta\mu_{III}$
Zn$_{III}^0$	$+0.52$	$+0.43$	$-\Delta\mu_{Zn}+\Delta\mu_{III}$
Cd$_{III}^0$	$+0.61$	$+0.89$	$-\Delta\mu_{Cd}+\Delta\mu_{III}$
Mg$_{Cu}^+$	$-2.12(-2.20)$	$-1.81(-1.90)$	$-\Delta\mu_{Mg}+\Delta\mu_{Cu}+(E_v+E_F)$
Zn$_{Cu}^+$	$-1.01(-1.08)$	$-0.77(-0.86)$	$-\Delta\mu_{Zn}+\Delta\mu_{Cu}+(E_v+E_F)$
Cd$_{Cu}^+$	$-0.80(-0.90)$	$-0.38(-0.51)$	$-\Delta\mu_{Cd}+\Delta\mu_{Cu}+(E_v+E_F)$
Mg$_{III}^-$	$-0.52(-0.60)$	$-0.35(-0.43)$	$-\Delta\mu_{Mg}+\Delta\mu_{III}-(E_v+E_F)$
Zn$_{III}^-$	$+0.57(+0.50)$	$+0.60(+0.50)$	$-\Delta\mu_{Zn}+\Delta\mu_{III}-(E_v+E_F)$
Cd$_{III}^-$	$+0.68(+0.61)$	$+1.05(+0.95)$	$-\Delta\mu_{Cd}+\Delta\mu_{III}-(E_v+E_F)$

TABLE IV. Formation energies ΔH of neutral and charged halogen donors and intrinsic defects. Values within bracket are the formation energies in the absent of the Makov-Payne correction.

	$\Delta H(D,q)$ [eV]		
	$[E(D,q)-E(0)]+\Sigma_\alpha n_\alpha \mu_\alpha^{solid}$		$\Sigma_\alpha n_\alpha \Delta\mu_\alpha + q(E_v + E_F)$
	CuInSe$_2$	CuGaSe$_2$	
V_{Cu}^0	+0.83	+0.63	$+\Delta\mu_{Cu}$
III$_{Cu}^0$	+0.90	+2.43	$-\Delta\mu_{III}+\Delta\mu_{Cu}$
Cl$_{Se}^0$	+0.51	+1.31	$-\Delta\mu_{Cl}+\Delta\mu_{Se}$
Br$_{Se}^0$	+0.54	+1.43	$-\Delta\mu_{Br}+\Delta\mu_{Se}$
I$_{Se}^0$	+0.73	+1.77	$-\Delta\mu_{I}+\Delta\mu_{Se}$
V_{Cu}^-	+0.90(+0.85)	+0.71(+0.61)	$+\Delta\mu_{Cu}-(E_v+E_F)$
III$_{Cu}^+$	0.01(−0.06)	+1.07(+1.01)	$-\Delta\mu_{III}+\Delta\mu_{Cu}+(E_v+E_F)$
III$_{Cu}^{++}$	−0.73(−1.01)	0.05(−0.28)	$-\Delta\mu_{III}+\Delta\mu_{Cu}+2(E_v+E_F)$
Cl$_{Se}^+$	−0.40(−0.47)	−0.17(−0.26)	$-\Delta\mu_{Cl}+\Delta\mu_{Se}+(E_v+E_F)$
Br$_{Se}^+$	−0.36(−0.42)	−0.05(−0.14)	$-\Delta\mu_{Br}+\Delta\mu_{Se}+(E_v+E_F)$
I$_{Se}^+$	−0.18(−0.26)	+0.24(+0.14)	$-\Delta\mu_{I}+\Delta\mu_{Se}+(E_v+E_F)$

should be as high as possible in the gap. At this point the intrinsic donors tend to compensate the intrinsic acceptors. Figure 4 shows the energy needed to form Ga$_{Cu}$ in CGS and In$_{Cu}$ in CIS. We see that $\Delta H(Ga_{Cu}) > \Delta H(In_{Cu})$. This reflects the larger band gap of CGS. Note from Fig. 4 that the self-consistently calculated E_F^{eq} is therefore higher in the gap for CIS than for CGS. Since, in the present case, the concentration of the ionized defects V_{Cu}^-, In$_{Cu}^{++}$ are much higher than the carrier concentration, E_F is pinned to the vicinity of the point

where the concentrations of the ionized defect alone yield charge balance. Due to the strong, i.e., exponential, dependence of the concentration on ΔH, this point is given by the lowest lying intersection point of donor and acceptor formation energies, $\Delta H(In_{Cu})=\Delta H(V_{Cu})$ defining $E_F^{n,comp}$ in Fig. 4. The exact value of the equilibrium Fermi level in the self-consistent solution is temperature dependent. It will, however, be pinned around $E_F^{n,comp}$. Significant deviation of the equilibrium $E_F(T)$ from $E_F^{n,comp}$ will be restored, because, e.g., for $E_F > E_F^{n,comp}$, the ΔH of the negatively charged defects (acceptors) becomes lower, increasing their concentration. The excess negative charge has to be compensated by a higher hole concentration, which requires that the Fermi level lowers again. The same argument, vice versa, holds for $E_F < E_F^{n,comp}$, so that E_F is pinned to $E_F^{n,comp}$.

C. Formation of wrong site defects and their electronic properties

The Fermi energy when $\Delta H(Cd_{Cu};E_F)=\Delta H(Cd_{In};E_F)$ is denoted $E_F^{n,site}$; ideally, it should be as high as possible in the gap. Figure 5 shows that it is lower in the gap in CGS than in CIS. Note that $E_F^{n,site}$ can be controlled by the chemical potential difference $\Delta\mu_{Cu}-\Delta\mu_{In}$. The smaller $\Delta\mu_{Cu}-\Delta\mu_{In}$, the higher $E_F^{n,site}$ will be in the energy gap due to easier Cd$_{Cu}$ formation and harder Cd$_{In}$ formation. This can be understood by comparing Fig. 3(a) and 3(e).

D. Electronic structure of Cd in CIS and CGS

Figure 6 compares the electronic structure of Cd-on-Cu to that of Cd-on-Ga in CGS. In pure CGS the valence band
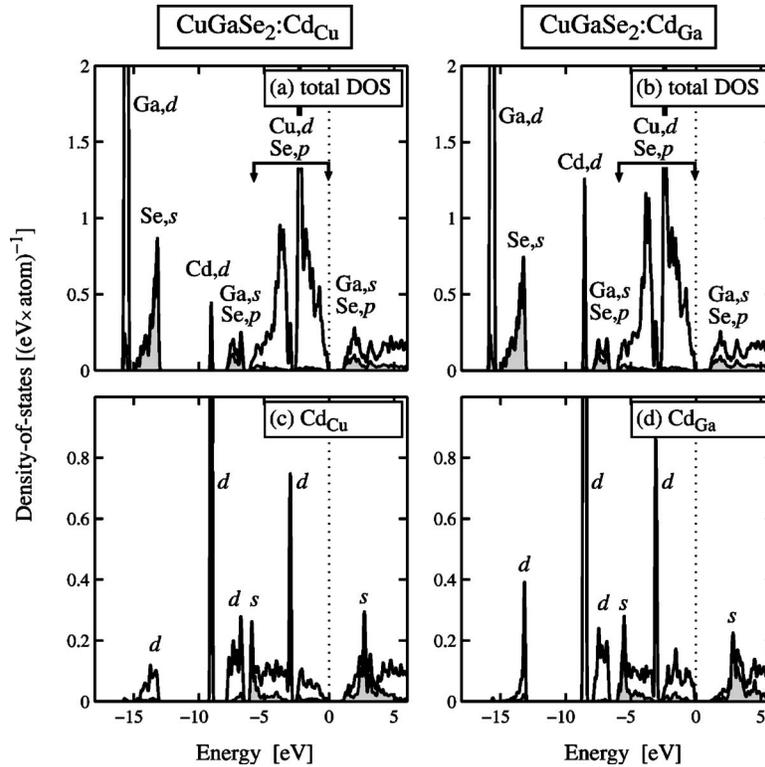
FIG. 6. Total DOS of (a) CGS:Cd$_{Cu}$ and (b) CGS:Cd$_{Ga}$, as well as the corresponding atom PDOS of the (c) Cd$_{Cu}$ and (d) Cd$_{Ga}$ dopant. The presented density-of-states includes a Gaussian broadening of 50 meV. Dotted lines indicate the VBM.

TABLE V. Transition energies $\varepsilon(D,q/q')$ of substitutional neutral and charged group-II donors and acceptors in CIS and CGS relative to the CBM, E_c, for the donors and to the VBM, E_v, for the acceptors. Values within bracket are the transition energies without the Makov-Payne correction.

	(q/q')	$\varepsilon(D,q/q')$ [eV]	
		CuInSe$_2$	CuGaSe$_2$
Mg$_{Cu}$	$(+/0)$	$E_c-0.14(-0.06)$	$E_c-0.11(-0.02)$
Zn$_{Cu}$	$(+/0)$	$E_c-0.14(-0.06)$	$E_c-0.20(-0.11)$
Cd$_{Cu}$	$(+/0)$	$E_c-0.10(-0.00)$	$E_c-0.18(-0.06)$
Mg$_{III}$	$(0/-)$	$E_v+0.13(+0.05)$	$E_v+0.15(+0.06)$
Zn$_{III}$	$(0/-)$	$E_v+0.05(-0.02)$	$E_v+0.17(+0.07)$
Cd$_{III}$	$(0/-)$	$E_v+0.07(+0.00)$	$E_v+0.16(+0.07)$

occurs between E_v and E_v-5 eV and has two peaks: the deeper one is bonding Cu, d-Se, p and the upper one is antibonding Cu, d-Se, p. The conduction band is made of Ga, s-Se,p orbitals. Deeper in the valence band we find the Ga, s-Se, p bonding states (E_v-6 eV); the Se s-band (E_v-14 eV), and the Ga $3d$ band (E_v-16 eV).

The projected density of states (PDOS) of the Cd$_{Cu}^0$ and Cd$_{Ga}^0$ show strong similarities, with Cd,d-like resonance state at $\sim(E_v-9.0)$ eV. This is consistent with the atomic Cd, $4d$-states which are ~7 eV below the Cu,$3d$-states and ~5 eV above the Ga,$3d$-states. The Cd,d-Se,p interaction yield pronounced Cd,d-like peaks also at $\sim(E_v-13.5)$ eV and $\sim(E_v-3.0)$ eV. The PDOS of the Cd$_{Cu}^0$ donor electron states at $\sim(E_v+2.5)$ eV is well above the experimental band-gap energy of 1.68 eV. This indicates a shallow character of the Cd$_{Cu}$ donor. The acceptor Cd$_{Ga}^0$, has its acceptor hole states at the VBM [the s-like states at $\sim(E_v+2.5)$ eV are unoccupied]. The PDOS of Cd$_{Ga}$ show stronger PDOS at the VBM, than of that of the Cd$_{Cu}$ donor.

V. TRANSITION ENERGIES

Table V shows the calculated transition energies according to Eq. (11). They are depicted graphically in Fig. 7. In Fig. 7, we do not include the Makov-Payne correction since the defect levels calculated here are rather shallow, and thus the truncated multipole expansion[18] is no good for the image charge correction.

In Fig. 7, we show schematically the transition energies of divalent doping of donors $\varepsilon(II_{Cu},0/+)$ and acceptors $\varepsilon(II_{III},-/0)$. The trend is that CGS has somewhat deeper group-II donors than CIS, and this trend is more pronounced for the group-II acceptors. However, the calculated transition energies indicates that the group-II donors could be thermally ionized both in CIS and in CGS. The multipole correction gives ~0.1 eV deeper donor and acceptor level since the correction increase the formation energy for charged states. The multipole correction is probably somewhat overestimated for shallow defect, and one would expect that the transition energies lies between the values with and without this correction.
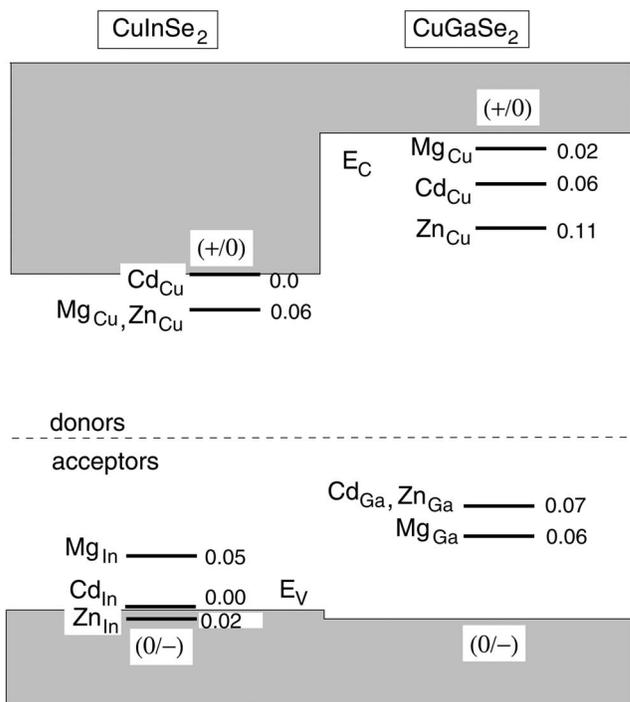
FIG. 7. Schematic picture of the transition energies (in units of eV) of divalent donors $(+/0)$ and acceptors $(0/-)$ in CIS and CGS, referenced to the CBM and VBM, respectively. The transition energy values shown are without Makov-Payne correction.

VI. DEFECT AND CARRIER CONCENTRATIONS: CAN CGS BE DOPED n-TYPE?

Having calculated the optimal chemical potential growth conditions (Secs. II C and II D), the formation energy (Sec. III A) and transition energy (Sec. III B), we can now calculate self-consistently the defect concentration and carrier concentration. They are shown for divalent doping in CIS and CGS in Fig. 8 and for halogen doping in Fig. 9. In case of Cd-doping of CIS under Se-poor ("point N") conditions, and using a Cd chemical potential corresponding to equilibrium with CdSe (maximal $\Delta\mu_{Cd}$), we find undesirably high Cd incorporation. Therefore, we used a slightly lower $\Delta\mu_{Cd}$ (by 0.2 eV).
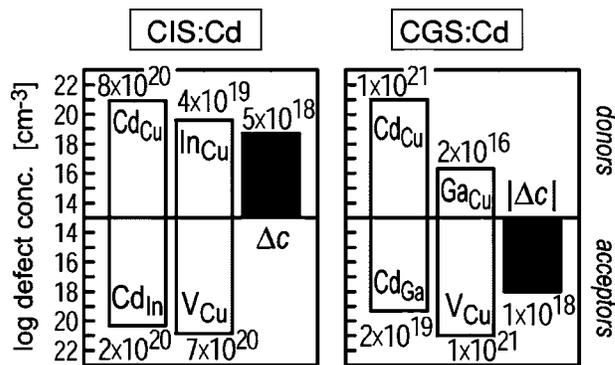
FIG. 8. The self-consistently calculated defect concentrations for Cd doping in CIS and CGS at $T=800$ K. The doping balance $\Delta c = c_{Cd_{Cu}} + 2c_{In_{Cu}} - c_{Cd_{In}} - c_{V_{Cu}}$ is shown in black bars.
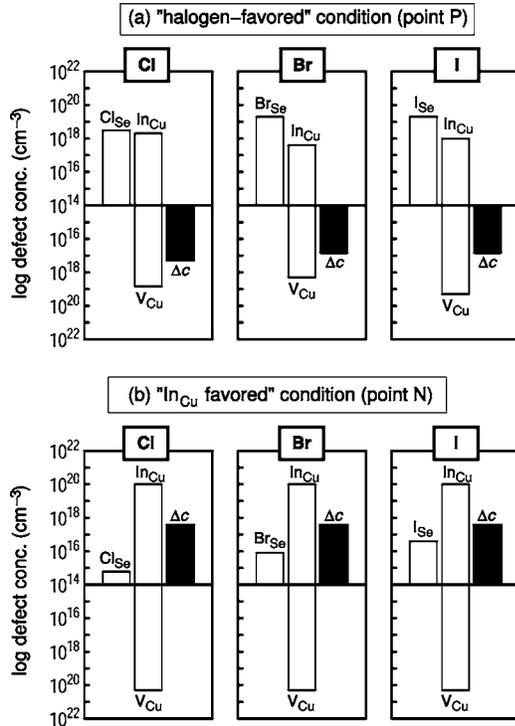
FIG. 9. The defect concentration of halogen defects and intrinsic defects under "halogen favored" (point P) and "In_{Cu} favored" (point N) conditions in CIS. The growth temperature of 800 K is used. The doping balance $\Delta c = c_{X_{Se}} + 2c_{In_{Cu}} - c_{V_{Cu}}$ (X represents halogen atoms) is shown in black bars.

Using $T = 800$ K,[19] the calculated concentrations for the "halogen favored" and the "In_{Cu} favored" conditions are shown as a bar chart in Figs. 9(a) and 9(b), respectively. Here, the doping balance, e.g., $\Delta c = c_{Cl_{Se}} + 2c_{In_{Cu}} - c_{V_{Cu}}$ for Cl-doping, indicates whether net donor doping ($\Delta c > 0$) or net acceptor doping ($\Delta c < 0$) is obtained under the respective conditions. We see that under "halogen favored" conditions [Fig. 9(a)], the halogen donors have concentrations of about 10^{19} cm^{-3}, but are overcompensated by Cu vacancies. The sample ends up being p-type with net acceptor concentrations in the 10^{17} cm^{-3} range [cf. Fig. 9(a)].

Under the "In_{Cu} favored" conditions, we find that the concentrations of the intrinsic defects In_{Cu} and V_{Cu} are practically independent on the type of the halogen dopant, being present in only low concentration, halogen $c_{halogen} \lesssim 10^{17}$ cm^{-3} [Fig. 9(b)]. In fact, $c_{In_{Cu}} = 2 \times 10^{20}$ cm^{-3} and $c_{V_{Cu}} = 3 \times 10^{20}$ cm^{-3} are practically equal to the concentrations obtained under Se-poor conditions without additional halogen doping, and show a high compensation ratio. The sample ends up being n-type with a net donor concentration of $\Delta c = 10^{18}$ cm^{-3} [Fig. 9(a)]. In order to determine the resulting free electron concentration at room temperature,[22] we perform another self-consistent calculation, now for $T = 300$ K, but maintaining the total concentrations of In_{Cu} and V_{Cu} obtained for 800 K. The calculated carrier concentration is $c_e \approx 2 \times 10^{14}$ cm^{-3}, meaning that only a relatively small fraction of electrons are thermally activated into the conduction band. This is a consequence of the high compensation ratio and the ensuing very high total (neutral + ionized) con-

centration of donors. The calculated carrier concentration is somewhat below the range of experimentally observed electron concentrations[23] $5 \times 10^{15} - 1.5 \times 10^{17}$ cm^{-3}, probably because of a slight overestimation of the ionization energies within the LDA supercell approach.

We find that the calculated electron concentrations at room temperature are much lower than the net donor concentrations, i.e., $c_e \approx 2 \times 10^{14}$ cm^{-3} in the case of Cl and intrinsic doping, and $c_e \approx 2 \times 10^{15}$ cm^{-3} in the case of Cd doping of CIS. These numbers are below the maximal electron concentrations observed after Cl and intrinsic n-type doping, and after Cd doping, being about 10^{17} cm^{-3} and 10^{18} cm^{-3}, respectively. We attribute this discrepancy mostly to a slight overestimated of the donor ionization energies within the LDA supercell approach. Nevertheless, these results qualitatively explain why the limit $c_e \approx 10^{17}$ cm^{-3} of intrinsic doping can be exceeded by Cd doping, but not by Cl doping.

Since our calculated formation energies indicated that equilibrium n-type doping by Cl or Cd can be achieved in CIS but not in pure CGS, we now address the question whether n-type doping can be achieved under equilibrium conditions with any other donor dopant. The growth conditions discussed here ("point N") are Cu-rich in the sense of a maximal $\Delta\mu_{Cu}$ (equilibrium with Cu-metal). This maximizes the formation energy of the electron killer V_{Cu}, minimizing its concentration. Still, $\Delta H(V_{Cu})$ is rather low, and $E_F^{n,pin}$ the Fermi level where $\Delta H(V_{Cu}^-) = 0$ [cf. Figs. 4 and 5], lies in the lower part of the CGS band gap. $E_F^{n,pin}$ defines an upper bound for the equilibrium Fermi energy E_F^{eq}, because $E_F^{eq} > E_F^{n,pin}$ would correspond to a situation where donor and acceptor formation energies intersect at a negative ΔH. In such a case the CGS host material would no longer be stable, e.g. if $\Delta H(Cd_{Cu}^+)$ and $\Delta H(Cd_{Ga}^-)$ would intersect at negative ΔH, the spontaneous substitution of Cu and Ga sites by Cd would lead to CdSe formation. Since $E_F^{n,pin}$ defines the maximal equilibrium Fermi energy, its position in the lower part of the band gap of CGS indicates that n-type doping under equilibrium conditions cannot be obtained in CGS, irrespective of the used donor species. In any case, donor doping is overcompensated by the electron-killer V_{Cu}.

VII. SUMMARY

We conclude that (i) the halogen incorporation is limited by chemical potential bounds imposed by precipitation of Cu- and In-halides and, hence, halogen incorporation is overwhelmed by the doping effect of the abundant intrinsic defects In_{Cu} and V_{Cu}. (ii) The formation of the intrinsic In_{Cu} double donor in CIS under Se-poor growth conditions results in net n-type doping. (iii) Due to the low formation energy of the compensating acceptor V_{Cu}, even at Cu-rich conditions $\Delta\mu_{Cu}$, a high degree of compensation will always be present for n-type doping in CIS. (iv) Under Se-poor conditions, which simultaneously imply Cu- and In-rich conditions, the Cu-site defect concentrations (V_{Cu}, In_{Cu}) are in the 10^{20} cm^{-3} range (Fig. 9b), meaning that several percent of the Cu sites are not occupied by Cu. Thus, CIS is highly nonstoichiometric Cu-poor even at this "Cu-rich" ($\Delta\mu_{Cu} = 0$) growth condition. (v) Due to the fact that $\Delta H(V_{Cu}^-)$ becomes zero in CGS
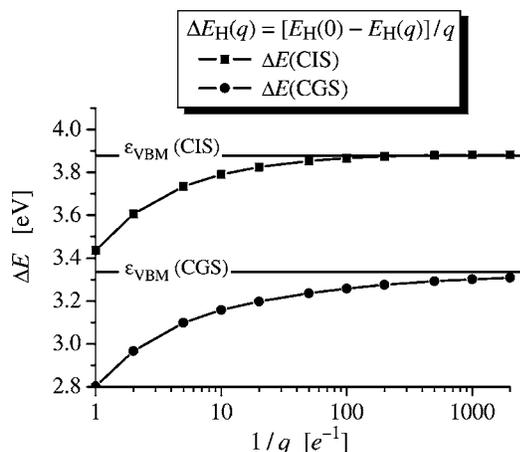
FIG. 10. Total energy difference ΔE per hole between the neutral semiconductor host and the positively charged (q) host, accomodating a hole gas in the valence band. The calculation is done for the 8 atom elementary cell of CIS and CGS. $1/q = 1000$ corresponds to a hole concentration of about 5×10^{18} cm^{-3}.

already at a low value of $E_F = 0.7$ eV , it is not possible to shift E_F to higher values under equilibrium conditions. Thus, future attempts should focus on nonequilibrium conditions, in which the atomic Cu reservoir is decoupled.

APPENDIX : TECHNICAL DETAILS ON HOW TO CALCULATE DEFECTS ENERGIES IN THE LDA SUPERCELL APPROACH

Determining the valence-band maximum

In this section, we show how the energy of the VBM, E_v, in Eq. (2) is determined from the total energy of the charged pure host crystal: The formation energy of charged defects depends on the Fermi energy. In a nondegenerate system, the Fermi energy lies in the band-gap energy region. It is, therefore, convenient to determine the energy of the VBM, E_v, and regard the Fermi energy E_F as a free parameter $0 \leq E_F \leq E_g$.

We define the energy of the VBM, E_v, as the energy difference between the pure host crystal with and without a hole at the VBM, i.e.,

$$\Delta E_H(q) = [E_H(0) - E_H(q)]/q, \tag{A1}$$

where q is the number of electrons removed in the calculation of the charged host. In the nondegenerate case, the energy of the VBM corresponds to that of a dilute hole gas, and one thus has to take $E_v = \lim_{q \to 0} \Delta E_H(q)$, or, equivalently, increasing the supercell size to infinity with $q=1$. Figure 10 shows the energy difference defined in Eq. (A1) as a function of $1/q$ in an 8 atom unit cell of CIS and CGS. Obviously, the energy difference $\Delta E_H(q)$ converges in the limit of a dilute

hole gas to the Kohn-Sham eigenvalue of the VBM, ϵ_{VBM}. Thus we may set $E_v = \epsilon_{VBM}$ for the calculation of ΔH in Eq. (2). Here, the problem is, however, that ϵ_{VBM} depends on the unknown average potential, and is defined only up to a constant. For consistency between the charged defect total energy $E_D(q \neq 0)$ and the energy of the VBM, ϵ_{VBM}, it is required to align the average potentials of the pure host and host + defect calculations. This is described in Sec. 4 of the Appendix.

LDA energy gap error

LDA is believed to accurately describe the total energy of pure intrinsic semiconductors. However, the LDA underestimates the fundamental band-gap energies of semiconductors by $\sim 50\%$. This LDA error will also be reflected in those impurity single-particle eigenstates which are in or above the energy region of the band gap. For intrinsic semiconductors, the LDA band-gap error is not a problem since the total ground state energy does not depends on the conduction band energy states. Of course, the problem can be avoided by using calculations beyond LDA, such as the GW method, where this problem is not present. However, the calculations beyond LDA currently are not feasible for defect calculations so far, and we must therefore find some reasonable approach for this band-gap correction based on LDA calculations.

In the first-order approximation, the energy correction of the fundamental band gap consists of of constant downward energy shift $\Delta E_v \geq 0$ of the valence bands and a constant upwards energy shift $\Delta E_c \geq 0$ of the conduction bands. The total correction of the band gap is (cp. Fig. 11)

$$\Delta E_g = \Delta E_c + \Delta E_v = E_g^{\mathrm{Expt}} - E_g^{\mathrm{LDA}} \tag{A2}$$

In this work, we assume that *shallow donor levels* follow the energy correction of the CBM, whereas *shallow acceptor levels* only follow energy correction of the VBM. That is, we assume that an energy correction consisting of shifting the conduction bands higher in energy will affect those shallow delocalized donor states which are energetically located near or above the CBM. Similarly, an energy correction consisting of shifting the valence bands lower in energy will affect those shallow delocalized acceptor states which are energetically located near or below the VBM. The energy correction of the occupied donor or acceptor states will affect the total energy containing the defect. Thus, for shallow donors one has to correct the LDA total energies by the same energy required to correct the single-particle energies for host electrons in the CBM, and for shallow acceptors one has to correct the LDA total energies by the same energy required to correct the single-particle energies for host holes in the VBM, i.e.,

$$\Delta E_g(D,q) = \begin{cases} z_e(D,q)\Delta E_c; & \text{donors} \\ z_h(D,q)\Delta E_v; & \text{acceptors}, \end{cases} \tag{A3}$$

where $z_e(D,q) = \Sigma_{j,\mathbf{k}} w_{\mathbf{k}} \eta_{j\mathbf{k}}$ is the number of donor electrons occupying the donor states near or above the host CBM. Here, the sum index are energy levels (j) and k-points $(\mathbf{k})$, and w_k represents the weight at the reciprocal point $\mathbf{k}$ while

$\eta_{j\mathbf{k}}$ is the electron occupation number at level j, reciprocal point $\mathbf{k}$. For example: $z_e(D,q)=1$ for shallow neutral divalent donors (e.g., Zn_{Cu}^0), while $z_e(D,q)=0$ for shallow charged divalent donors (e.g., Zn_{Cu}^+), and $z_e(D,q)=2$ for shallow neutral double donors (e.g., Ga_{Cu}^0), and $z_e(D,q)=1$ for shallow partially charged ($q=+$) double donors (e.g., Ga_{Cu}^+), and $z_e(D,q)=0$ for shallow charged ($q=++$) double donors (e.g., Ga_{Cu}^{++}). Analogously, $z_h(D)$ is the number of acceptor holes occupying the acceptor states near or below the host VBM.

If the VBM is shifted downward by ΔE_v, one also has to shift the reference energy E_v in Eqs. (2) and (11) by

$$E_v = E_v^{LDA} - \Delta E_v, \tag{A4}$$

and this correction will affect the formation energy of charged defects due to the term $q(E_v+E_F)$ in Eq. (2).

Band filling correction

The formation and transition energies of dopants are normally referenced to a doping concentration in the dilute limit i.e., $\ll 10^{18}$ cm^{-3}. However, for a single defect in a finite supercell calculation, the defect concentration is much higher, e.g., $\sim 10^{21}$–10^{22} cm^{-3} in a 64-atom supercell. The high doping concentration implies an unwanted impurity-impurity interaction. Due to this interaction, the impurity electrons form a impurity band instead of a single localized electron state. This incorrect impurity band dispersion need to be compensated to obtain the total energy of the crystal with a defect concentration in the dilute limit. Moreover, if the impurity band is energetically above or close to the host conduction (or valence) bands, then the impurity band can easily hybridize with the host electron states, and the donor electrons can partly populate the host conduction bands (cp Fig. 11). Thus, one needs to take into account possible band filling of the host energy bands. To correct the total energy $E(D,q)$ of the finite supercell due to this band-filling effects, one has to subtract the higher energy populations. For charged shallow donors, the correction is

$$\Delta E_{bf}(D,q) = - \sum_{j \geqslant c, \mathbf{k}} (w_{\mathbf{k}} \eta_{j\mathbf{k}} \varepsilon_{j\mathbf{k}} - \varepsilon_{c\mathbf{0}}). \tag{A5}$$

Here, $\varepsilon_{j\mathbf{k}}$ is the single-particle eigenstates of the donor electrons, and $\varepsilon_{c\mathbf{0}}$ is for shallow donors the lowest populated donor electron state, normally located at the Γ-point. The weights $w_{\mathbf{k}}$ of the $\mathbf{k}$-points are determined from the $\mathbf{k}$-mesh, and the weights $\eta_{j\mathbf{k}}$ of the electron population are obtained from the tetrahedron $\mathbf{k}$-space integration.[14]

In Eq. (A5) we assume that the electron state $\varepsilon_{c\mathbf{0}}$ is energetically close to the single populated electron state in the dilute limit. This is true for very shallow donor levels which has most of their energy states well above the CBM, but it might be less accurate assumption for less shallow donor states which strongly hybridize with the CBM.

The correction to the band-dispersion and band-filling effects is a consequence of employing the finite supercell approach for the calculation of the total energy of systems in the dilute limit. However, if one aims to calculate the total energy of highly doped semiconductors, the correction of Eq. (A5) should be zero (or at least smaller) since band distortion and heavily band filling should be present in those systems.

Potential alignment correction of charged defects (any cell size)

In a momentum-space formalism with periodic boundary conditions, the violation of the charge neutrality condition, which occurs for the calculation of charged defect states, leads to the divergence of the Coulomb potential. Usually, one circumvents this problem by setting the $\mathbf{G}=\mathbf{0}$ component of the electrostatic potential $V_H(\mathbf{G}=\mathbf{0})$ to zero. As a consequence, the spectrum of the Kohn-Sham eigenvalues is defined only up to a constant. The value of the constant offset is, in general, not known and depends on the average crystal potential and the choice of pseudopotential (e.g., hard or soft). Despite this arbitrariness of the eigenvalues, the total energy of a charge neutral system is well-defined, because the neglect of the constant offset in the eigenvalue sum is counterbalanced by other terms in the total energy expression.[24] As shown in Fig. 10, the total energy difference of the pure host in the neutral and positively charged state (modeling a hole in the valence band) converges to the eigenvalue of the VBM. Thus, the total energy of the charged system, calculated with the total energy expression which was originally derived for a charge neutral system, is obviously subject to the same arbitrariness as the eigenvalue spectrum. It is emphasized that the nonuniqueness of the total energy of charged supercells is a consequence of the periodic boundary conditions and would not occur in a finite cluster calculation, where the violation of charge neutrality constitutes no problem in principle. Clearly, the development of a unique total energy expression for charged periodic systems would be desirable.

Since the unknown offset occurs at two places, namely for the calculation of E_v and for the energy $E(D,q)$ of the charged defect [see Eq. (2)], one needs to make sure that these energies are consistent with respect to potential alignment. Introducing a charged defect into a supercell can change the average potential significantly, resulting in a shift of the eigenvalues, even of those corresponding to states of host atoms far from the defect. In order to achieve consistency, the potentials of the charged defect and the host calculation have to be aligned. The total energy of a charged defect is then corrected by

$$\Delta E_{pa}(D,q) = q \cdot [V_R(D,q) - V_R(0)], \tag{A6}$$

where $[V_R(D,q)-V_R(0)]$ is the difference of the potential at a reference point in the defect and the host calculations. In order to determine the potential alignment, one can monitor either (i) the eigenvalues of localized states at host atoms far from the defect, or (ii) the electrostatic potential preferably at interstitial sites far from the defect.

Image charge correction, due to finite supercell (charged defects only)

Calculation of the energy of a charged system is of interest for charged impurities in crystalline solids. However, the
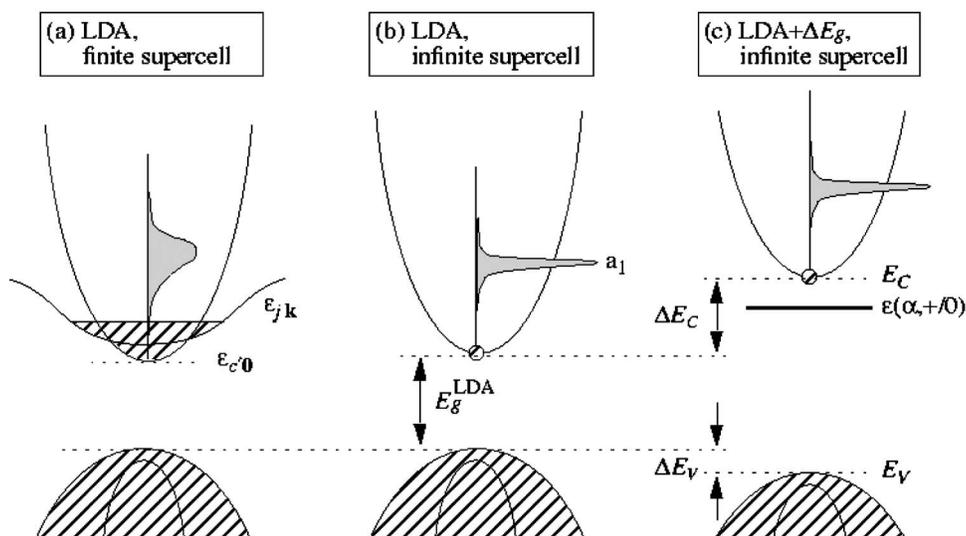
FIG. 11. Schematic figure showing the (a) band-filling correction to the (b) LDA finite supercell approach, and (c) the band-gap corrections. The shaded area show schematically the density-of-states of the donor electron *s*- states.

energy of a periodically repeated electrically charged system diverges, and thus a jellium background is adopted to neutralize the charge in general. Makov and Payne[18] argued that the charge density in a crystalline solid with a point defect can be the sum of two contributions—the periodic charge density of the underlying crystalline solid and the charge density of the aperiodic defect, which is the charge difference between with and without the defect. The multipole correction ΔE_{mp} of the total energy of a practical finite supercell with respect to the total energy of an ideal infinite cell of a charged aperiodic system is[18]

$$\Delta E_{mp}(D,q) = +\frac{q^2\alpha_M}{2\varepsilon_0 V_c^{1/3}} + \frac{2\pi qQ}{3\varepsilon_0 V_c} + O(V_c^{-5/3}). \quad (A7)$$

Here, α_M is the lattice-dependent Madelung constant and V_c is the volume of the cubic supercell. ε_0 and Q are properties of the periodic density and the aperiodic density; ε_0 is the static dielectric constant and Q is the second radial moment only of that part of the aperiodic density. The first and second correction terms in Eq. (A7) are the monopole and quadrupole corrections, respectively. Typically, the quadrupole correction is ~30% of the monopole correction with opposite sign. In principal, also higher order of the multipole correction should be included.

We notice that Eq. (A7) is based on the assumption that defect charge is rather localized. However, the defect charge of very shallow levels might be rather delocalized, and the restriction to monopole and quadrupole corrections in Eq. (A7) may not be sufficient, i.e., higher order terms may be needed. In the limit of completely delocalized charges, the multipole correction should be zero since an uniform electron gas does not have a net charge moment. One can therefore argue that the Makov-Payne correction is the upper limit of correction for shallow defects. We therefore present the formation and transition energies both with and without the multipole correction.

As in the case of the correction for the band-filling (see above), the multipole correction should be zero (or at least smaller) if one intentionally calculates total energies of heavily doped semiconductors. For those highly doped systems, the choice of assuming periodic instead of, for instance, randomly distributed donors may however have an effect on the impurity-impurity interaction.

With the corrections above, the total energy of the crystal with a defect is

$$E(D,q) = E_{FSC}^{LDA}(D,q) + \Delta E_{bf}(D,q) + \Delta E_{mp}(D,q) + \Delta E_{pa}(D,q)$$
$$+ \Delta E_g(D,q), \quad (A8)$$

where $E_{FSC}^{LDA}(D,q)$ is the LDA total energy of the finite supercell with the defect (see Fig. 11).

*Present address: Department of Materials Science and Engineering, Royal Institute of Technology, SE-100 44 Stockholm, Sweden

[1] D. Lillington, H. Cotal, J. Ermer, D. Friedman, T. Moriarty, and A. Duda, *35th Intersociety Energy Conversion Engineering Conference*, July, 2000, Las Vegas, NV, USA, Vol. 1, p. 516.

[2] K. Ramanathan, M. A. Contreras, C. L. Perkins, S. Asher, F. S. Hasoon, J. Keane, D. Young, M. Romero, W. Metzger, R. Noufi *et al.*, Prog. Photovoltaics **11**, 225 (2003).

[3] C. Heske, D. Eich, R. Fink, E. Umbach, T. van Buuren, C. Bostedt, L. J. Terminello, S. Kakar, M. M. Grush, T. A. Callcott *et al.*, Appl. Phys. Lett. **74**, 1451 (1999).

[4] D. Liao and A. Rockett, J. Appl. Phys. **93**, 9380 (2003).

[5] T. Nakada, K. Furumi, K. Sonoda, and A. Kumioka, *2nd World Conference and Exhibition on Photovoltaic Solar Energy Conversion*, Hofbur, Kongresszentrum, Wien, Austria, July, 1998.

[6] K. Ramanathan, F. S. Hasoon, S. Smith, A. Mascarenhas, H. Al-Thani, J. Alleman, H. S. Ullal, J. Keane, P. K. Johnson, and J. R. Sites, *Twenty-Ninth IEEE Photovoltaic Specialists Conference 2002*, May 2002, New Orleans, LA, USA, p. 523.

[7] S. B. Zhang and S.-H. Wei, Appl. Phys. Lett. **80**, 1376 (2002).

[8] S. B. Zhang and J. E. Northrup, Phys. Rev. Lett. **67**, 2339 (1991).

[9] S. B. Zhang, S.-H. Wei, A. Zunger, and H. Katayama-Yoshida, Phys. Rev. B **57**, 9642 (1998).

[10] A. Zunger, Appl. Phys. Lett. **83**, 57 (2003).

[11] C. P. J. M. van der Vorst, G. C. Verschoor, and W. J. A. Maaskant, Acta Crystallogr., Sect. B: Struct. Crystallogr. Cryst. Chem. **34**, 3333 (1978).

[12] Http://www.webelements.com.

[13] The formation energy of In_2Se_3 and Ga_2Se_3 in tetragonal (instead of the hexagonal ground structure) are used according to Ref. 9. This will not affect the colored area in Fig. 2, although the stable chemical potential regions for the ordered defect structure of teneries are increased in comparison to the use of ground structure of In_2Se_3 and Ga_2Se_3.

[14] G. Kresse and J. Hafner, Phys. Rev. B **47**, R558 (1993); G. Kresse and J. Furthmüller, *ibid.* **54**, 11 169 (1996).

[15] J. P. Perdew and A. Zunger, Phys. Rev. B **23**, 5048 (1981).

[16] J. E. Jaffe and A. Zunger, Phys. Rev. B **29**, 1882 (1984).

[17] L. Ley, R. A. Pollak, F. R. McFeely, S. P. Kowalczyk, and D. A. Shirley, Phys. Rev. B **9**, 600 (1974).

[18] G. Makov and M. C. Payne, Phys. Rev. B **51**, 4014 (1995).

[19] A. M. Gabor, J. R. Tuttle, D. S. Albin, M. A. Contreras, R. Noufi, and A. M. Hermann, Appl. Phys. Lett. **65**, 198 (1994).

[20] Instead of using the simplification $n \cdot p = \exp(-E_g/KT)$, as used in most textbook examples, the Fermi-Dirac distribution function is integrated directly. Accordingly, there is no assumption necessary that E_F is separated from the band edges by $\Delta E \gg kT$.

[21] S. B. Zhang, S.-H. Wei, and A. Zunger, J. Appl. Phys. **83**, 3192 (1998).

[22] Deepak and A. Priyadarshi, Mater. Sci. Eng., B **94**, 20 (2002).

[23] S. M. Wasim, Sol. Cells **16**, 289 (1986).

[24] J. Ihm, A. Zunger, and M. L. Cohen, J. Phys. C **12**, 4409 (1979).